Preprint typeset in JINST style - HYPER VERSION

arXiv:1411.1433v2 [physics.ins-det] 15 Jun 2015

Radiopurity assessment of the tracking readout for the NEXT double beta decay experiment

S. Cebrián,[a,b*] J. Pérez,[c] I. Bandac,[b] L. Labarga,[d] V. Álvarez,[e] A.I. Barrado,[f] A. Bettini,[b,g] F.I.G.M. Borges,[h] M. Camargo,[i] S. Cárcel,[e] A. Cervera,[e] C.A.N. Conde,[h] E. Conde,[f] T. Dafni,[a,b] J. Díaz,[e] R. Esteve,[j] L.M.P. Fernandes,[h] M. Fernández,[f] P. Ferrario,[e] A.L. Ferreira,[k] E.D.C. Freitas,[h] V.M. Gehman,[l] A. Goldschmidt,[l] J.J. Gómez-Cadenas,[e†] D. González-Díaz,[a,b] R.M. Gutiérrez,[i] J. Hauptman,[m] J.A. Hernando Morata,[n] D.C. Herrera,[a,b] I.G. Irastorza,[a,b] A. Laing,[e] I. Liubarsky,[e] N. López-March,[e] D. Lorca,[e] M. Losada,[i] G. Luzón,[a,b] A. Marí,[j] J. Martín-Albo[e] A. Martínez,[e] G. Martínez-Lema,[n] T. Miller,[l] F. Monrabal,[e] M. Monserrate,[e] C.M.B. Monteiro,[h] F.J. Mora,[j] L.M. Moutinho,[k] J. Muñoz Vidal,[e] M. Nebot-Guinot,[e] D. Nygren,[l] C.A.B. Oliveira,[l] A. Ortiz de Solórzano,[a,b] J.L. Pérez Aparicio,[o] M. Querol,[e] J. Renner,[l] L. Ripoll,[p] J. Rodríguez,[e] F.P. Santos,[h] J.M.F. dos Santos,[h] L. Serra,[e] D. Shuman,[l] A. Simón,[e] C. Sofka,[q] M. Sorel,[e] J.F. Toledo,[j] J. Torrent,[p] Z. Tsamalaidze,[r] J.F.C.A. Veloso,[k] J.A. Villar,[a,b] R.C. Webb,[q] J.T. White,[q] N. Yahlali[e]

[a] *Laboratorio de Física Nuclear y Astropartículas, Universidad de Zaragoza*
Calle Pedro Cerbuna 12, 50009 Zaragoza, Spain
[b] *Laboratorio Subterráneo de Canfranc*
Paseo de los Ayerbe s/n, 22880 Canfranc Estación, Huesca, Spain
[c] *Instituto de Física Teórica (IFT), UAM/CSIC*
Campus de Cantoblanco, 28049 Madrid, Spain
[d] *Departamento de Física Teórica, Universidad Autónoma de Madrid*
Campus de Cantoblanco, 28049 Madrid, Spain
[e] *Instituto de Física Corpuscular (IFIC), CSIC & Universitat de València*
Calle Catedrático José Beltrán, 2, 46980 Paterna, Valencia, Spain
[f] *Centro de Investigaciones Energéticas, Medioambientales y Tecnológicas (CIEMAT)*
Complutense 40, 28040 Madrid, Spain
[g] *Padua University and INFN Section, Dipartimento di Fisca G. Galilei, Via Marzolo 8, 35131 Padova, Italy*
[h] *Departamento de Fisica, Universidade de Coimbra*
Rua Larga, 3004-516 Coimbra, Portugal
[i] *Centro de Investigaciones en Ciencias Básicas y Aplicadas, Universidad Antonio Nariño*
Carretera 3 este No. 47A-15, Bogotá, Colombia
[j] *Instituto de Instrumentación para Imagen Molecular (I3M), Universitat Politècnica de València*
Camino de Vera, s/n, Edificio 8B, 46022 Valencia, Spain
[k] *Institute of Nanostructures, Nanomodelling and Nanofabrication (i3N), Universidade de Aveiro*
Campus de Santiago, 3810-193 Aveiro, Portugal
[l] *Lawrence Berkeley National Laboratory (LBNL)*
1 Cyclotron Road, Berkeley, California 94720, USA
[m] *Department of Physics and Astronomy, Iowa State University*
12 Physics Hall, Ames, Iowa 50011-3160, USA
[n] *Instituto Gallego de Física de Altas Energías (IGFAE), Univ. de Santiago de Compostela*
Campus sur, Rúa Xosé María Suárez Núñez, s/n, 15782 Santiago de Compostela, Spain
[o] *Dpto. de Mecánica de Medios Continuos y Teoría de Estructuras, Univ. Politècnica de València*
Camino de Vera, s/n, 46071 Valencia, Spain
[p] *Escola Politècnica Superior, Universitat de Girona*
Av. Montilivi, s/n, 17071 Girona, Spain
[q] *Department of Physics and Astronomy, Texas A&M University*
College Station, Texas 77843-4242, USA
[r] *Joint Institute for Nuclear Research (JINR)*
Joliot-Curie 6, 141980 Dubna, Russia

ABSTRACT: The "Neutrino Experiment with a Xenon Time-Projection Chamber" (NEXT) is intended to investigate the neutrinoless double beta decay of ^{136}Xe, which requires a severe suppression of potential backgrounds; therefore, an extensive screening and selection process is underway to control the radiopurity levels of the materials to be used in the experimental set-up of NEXT. The detector design combines the measurement of the topological signature of the event for background discrimination with the energy resolution optimization. Separate energy and tracking readout planes are based on different sensors: photomultiplier tubes for calorimetry and silicon multi-pixel photon counters for tracking. The design of a radiopure tracking plane, in direct contact with the gas detector medium, was specially challenging since the needed components like printed circuit boards, connectors, sensors or capacitors have typically, according to available information in databases and in the literature, activities too large for experiments requiring ultra-low background conditions. Here, the radiopurity assessment of tracking readout components based on gamma-ray spectroscopy using ultra-low background germanium detectors at the Laboratorio Subterráneo de Canfranc (Spain) is described. According to the obtained results, radiopure enough printed circuit boards made of kapton and copper, silicon photomultipliers and other required components, fulfilling the requirement of an overall background level in the region of interest of at most 8×10^{-4} counts keV^{-1} kg^{-1} y^{-1}, have been identified.

KEYWORDS: Double beta decay; Time-Projection Chamber (TPC); Gamma detectors (HPGe); Search for radioactive material.

*Corresponding author (scebrian@unizar.es).
†Spokesperson (gomez@mail.cern.ch).

Contents

1. Introduction **1**

2. Measurements **3**

3. Results **6**

3.1 Printed Circuit Boards and cables 8

3.2 Connectors 10

3.3 Soldering materials 10

3.4 SiPMs 10

3.5 Other components 11

4. Conclusion **12**

1. Introduction

Double beta decay experiments are one of the most active research topics in Neutrino Physics. The observation of the neutrinoless mode, as a peak at the transition energy, could give unique information on the neutrino nature, showing that neutrinos are Majorana particles, and for the determination of their mass hierarchy (see for instance [1]-[3]). The current generation of experiments aims at detector target masses at the 100 kg scale, while the next generation will need to go to the ton scale in order to completely explore the inverse hierarchy models of neutrino mass [4]. Since double beta decay is a very rare process, an ultra-low background level at the region where the signal is expected to appear is one of the main experimental requirements for a successful experiment. The NEXT experiment ("Neutrino Experiment with a Xenon Time-Projection Chamber") aims to search for such a decay in ^{136}Xe at the Laboratorio Subterráneo de Canfranc (LSC) [5], located at the Spanish Pyrenees, with a source mass of $\sim$100 kg (NEXT-100 phase). NEXT takes a detector=source approach, with the double beta emitters inside the detector, in order to maximize signal detection efficiency and the accumulation of a large mass of the relevant isotope. The challenge of NEXT is to combine the measurement of the topological signature of the event (in order to discriminate the signal from background) with the energy resolution optimization (to single out the peak at the sum energy of the two emitted electrons). The NEXT detector will be a high pressure gaseous xenon Time-Projection Chamber (TPC) with proportional electroluminescent (EL) amplification [6]: light from the Xe electroluminescence generated at the anode is recorded both in the photosensor plane right behind it for tracking and in the photosensor plane behind the transparent cathode for a precise energy measurement. As illustrated in figure 1, the separate energy and tracking readout planes, located at opposite sides of the pressure vessel, will use different sensors: photomultiplier tubes (PMTs) for calorimetry (and for fixing the start of the event) and silicon photomultipliers (SiPMs)

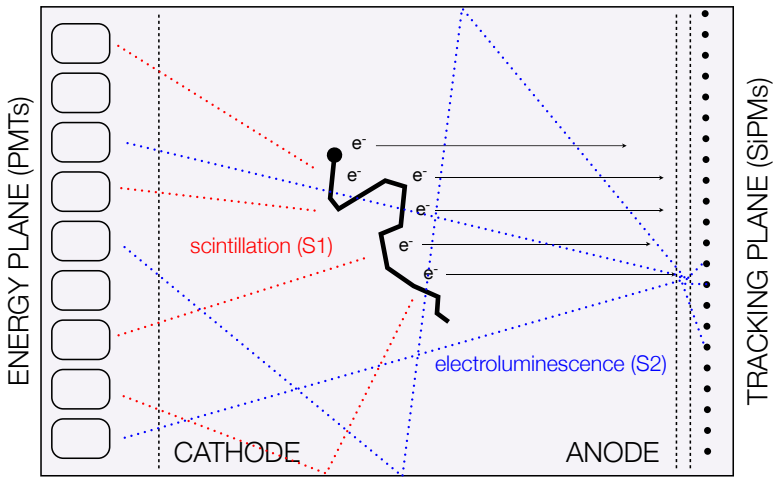

Figure 1. Concept of the NEXT experiment: light from the Xe electroluminescence generated at the anode is recorded both in the photosensor plane right behind it for tracking and in the photosensor plane behind the transparent cathode for a precise energy measurement. Primary scintillation defining the start of the event is also detected by the cathode photosensors.

for tracking. While work on prototypes is still ongoing [7]-[12], the installation of shielding and ancillary system started at LSC in 2013. Underground commissioning of the NEW detector begun at the end of 2014 and first data are expected along 2015. The NEW (NEXT-WHITE) apparatus[1] is the first phase of the NEXT detector to operate underground; it is a downscale 1:2 in size (1:8 in mass) of NEXT-100.

The goal of NEXT is to explore electron neutrino effective Majorana masses below 100 meV for a total exposure of 500 kg·year [1]. To reach this sensitivity, there are two basic requirements [13]: 1) An energy resolution of at most 1% FWHM at the transition energy ($Q_{\beta\beta}$ =2.458 MeV), which is reachable with EL amplification according to the results of prototypes [7, 14]. 2) A background level below 8×10^{-4} counts keV^{-1} kg^{-1} y^{-1} in the energy region of interest, achievable thanks to passive shieldings, background discrimination techniques based on charged particle tracking and a thorough material radiopurity control. The NEXT-100 shielding will consist of a 20-cm-thick lead castle covering the pressure vessel, suppressing by more than four orders of magnitude the external gamma radiation at the region of interest, together with an additional 12-cm-thick layer of copper inside the vessel intended to shield emissions from the vessel itself. The ability to discriminate signal from background is a powerful tool in NEXT. Signal events will appear uniformly distributed in the source volume of enriched xenon and will have a distinctive topology (a twisted long track, about 30 cm long at 10 bar, ending in two larger energy depositions). Defining a fiducial volume eliminates all charged backgrounds entering the detector while confined tracks generated by neutral particles, like high-energy gammas, can be suppressed by reconstructed topology of the events. Thus, the relevance of a background source depends on its probability of generating a signal-like track in the fiducial volume with energy around $Q_{\beta\beta}$. The

[1]The name honours the memory of the late Professor James White, key scientist of the NEXT project.

most dangerous background sources are then ^{208}Tl and ^{214}Bi, isotopes of the progeny of ^{232}Th and ^{238}U.

Concerning the radiopurity control, an extensive material screening and selection process for NEXT components is underway for several years. Determination of the activity levels is based on gamma-ray spectroscopy using ultra-low background germanium detectors at LSC and also on other techniques like Glow Discharge Mass Spectrometry and Inductively Coupled Plasma Mass Spectrometry. Materials to be used in the shielding, pressure vessel, electroluminescence and high voltage components, and energy and tracking readout planes have been taken into consideration and first results have been presented in [15, 16, 17]. These results are the input for the construction of a precise background model of the NEXT experiment based on Monte Carlo simulations, which is currently underway using the Geant4 code [18]; preliminary estimates indicate that shielding, vessel, field cage and energy plane could produce a background level of $\sim 4 \times 10^{-4}$ counts keV^{-1} kg^{-1} y^{-1} in the region of interest. The design of a radiopure tracking readout plane is complicated by the fact that printed circuit boards and electronic components, involving typically different composite materials, show in many cases activity levels too large for being used in experiments demanding ultra-low background conditions (see for instance [19] or [20]). SiPM technology offers an outstanding performance for photon detection [21], but scarce information on its radiopurity is available. According to simulations, a maximum activity of 70 mBq from ^{208}Tl and ^{214}Bi at the tracking plane could be tolerated, since it would generate other 4×10^{-4} counts keV^{-1} kg^{-1} y^{-1} in the region of interest. Therefore, an exhaustive screening program specifically for the tracking readout components was undertaken and is described here.

The tracking function in NEXT-100 detector will be provided by a plane of SiPMs operating as sensor pixels and placed behind the transparent EL gap (see figure 1), inside the pressure vessel. The SiPMs will be mounted in an a array of 107 square boards (named "Dice Boards", DB), to cover the whole field cage cross section. Each DB contains 8×8 SiPM sensors with a pitch of $\sim$1 cm between them; in addition, one NTC thermistor acting as temperature sensor is placed on the center of each DB and LEDs are included to allow a precise PMT geometrical calibration. As SiPMs provide very small current signals, the transmission of a high number of these signals from the photodetectors to the front-end electronics, crossing through the pressure vessel and traveling along several meters of cables, is not easy. The front-end electronics should be placed as close as possible to the detector; it will be located outside the lead shielding to minimize backgrounds from their non-radiopure components. The design of the tracking readout plane and front-end electronics has been tested in NEXT-DEMO [10, 22].

The structure of the paper is the following. Section 2 summarizes all the measurements performed, describing both the samples analyzed and the detectors used. Activity results obtained are collected in section 3, together with the discussion of implications for design and for the NEXT-100 background model. Finally, conclusions are drawn in section 4.

2. Measurements

The material screening program of the tracking readout of the NEXT experiment is based on germanium γ-ray spectrometry using ultra-low background detectors operated deep underground, at a

Table 1. Background counting rates (expressed in counts d^{-1} kg^{-1}) of the germanium detectors used at LSC for the NEXT tracking plane measurements. Integral rate from 100 to 2700 keV and rates at different peaks (583 keV from ^{208}Tl, 609 keV from ^{214}Bi and 1461 keV from ^{40}K) are presented. Only statistical errors are quoted.

Detector name	Mass (kg)	100-2700 keV	583 keV	609 keV	1461 keV
GeAnayet	2.183	714±3	3.73±0.40	1.76±0.28	0.31±0.20
GeAspe	2.187	441±2	3.77±0.47	3.74±0.45	0.58±0.24
GeLatuca	2.187	667±3	3.02±0.32	5.66±0.39	0.47±0.13
GeOroel	2.230	461±2	0.98±0.23	2.69±0.30	0.32±0.13
Paquito	1	79±2	0.27±0.09	0.48±0.21	0.25±0.13

depth of 2450 m.w.e., from the Radiopurity Service of LSC; being a non-destructive technique, the actual components to be used in the experiment can be analyzed.

The Radiopurity Service of LSC offers several detectors to measure ultra-low level radioactivity. They are p-type close-end coaxial 2.2-kg High Purity germanium detectors, from Canberra France, with aluminum or copper cryostats and 100-110% relative efficiencies[2]. Data acquisition is based on Canberra DSA 1000 modules and shielding consists of 5 or 10 cm of copper in the inner part surrounded by 20 cm of low activity lead, flushed with nitrogen gas to avoid airborne radon intrusion. The measurements related with the tracking readout were carried out at LSC using in particular four different $\sim$2.2 kg detectors from LSC (named GeAnayet, GeAspe, GeLatuca, and GeOroel) and also a $\sim$1 kg detector from the University of Zaragoza (named Paquito). For the measurements presented here, only GeAspe had a 10-cm-thick copper shield. Table 1 shows the counting rates of all the detectors used in the energy window from 100 to 2700 keV and at different peaks: 583 keV from ^{208}Tl, 609 keV from ^{214}Bi and 1461 keV from ^{40}K; all rates are expressed in counts per day and per kg of germanium detector. More details on detectors and their backgrounds can be found at [15, 23].

To derive the activity of an isotope producing a gamma emission of a certain energy in a sample, the main ingredients are the net signal (that is, the number of events at the gamma line stemming from the sample) and the full-energy peak detection efficiency at the corresponding energy. The criteria proposed in Currie's landmark paper [24] and revised in [25, 26] have been followed to evaluate net signals; activities have been quantified when possible and upper limits with a 95.45% C.L. have been derived otherwise. In the cases when the background from the experimental setup gives the dominant contribution to the gamma-line under evaluation, the gaussian limit has been taken in the statistical analysis of that line. Concerning the estimate of the detection efficiency, Monte Carlo simulations based on the Geant4 [27] code have been performed for each sample, accounting for intrinsic efficiency, the geometric factor and self-absorption at the sample. The configuration of each detector, including the germanium crystal, cryostat and components inside, is implemented in detail in the code following the manufacturer's specifications; the external copper and lead shielding is also considered. G4EmLivermorePhysics class is used to define the physics models for the simulation of the gamma emissions. Validation of the simulation

[2]Efficiency relative to a $3'' \times 3''$ NaI detector at 1332 keV and for a distance of 25 cm between source and detector.

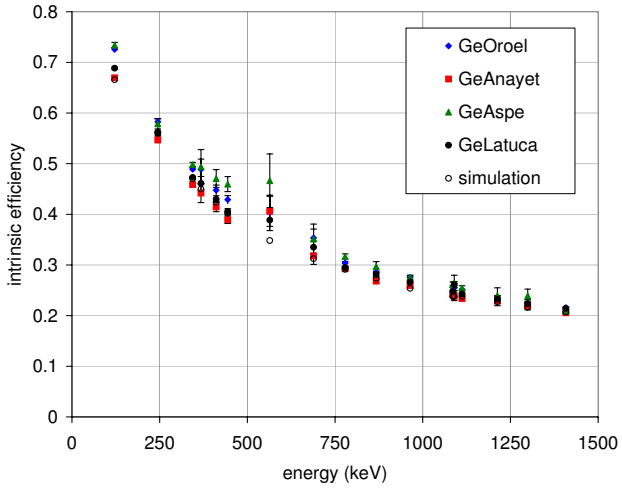

Figure 2. Intrinsic efficiency measured with a ^{152}Eu reference point source for the 2-kg germanium detectors of the Radiopurity Service of LSC used in the measurements and the corresponding simulation (for Anayet detector).

environment has been made by comparing the efficiency curve of each detector (measured with a ^{152}Eu reference point source of known activity located at a distance of 25 cm) with the simulated one. Figure 2 shows the intrinsic efficiency (corrected by solid angle) obtained for GeOroel, GeTobazo, GeAnayet and GeLatuca detectors together with a simulation considering GeAnayet geometry. The inclusion in the simulations of a dead layer over the whole crystal, with a thickness from 0.5 to 1 mm according to the detector specification sheets, has a non-negligible effect on the detector efficiency and allows to improve the agreement with measurements, especially at low energies, reducing deviations to a level of 5%. The relative efficiencies derived from measurements and simulation reproduce the values specified by the manufacturer. The overall uncertainty in the calculated detection efficiency of the samples for every gamma line is estimated to be 10%. The activity values and limits presented in table 3 are further affected by this uncertainty.

Activities of different sub-series in the natural chains of ^{238}U, ^{232}Th and ^{235}U as well as of common primordial, cosmogenic or anthropogenic radionuclides like ^{40}K, ^{60}Co and ^{137}Cs have been evaluated by analyzing the most intense gamma lines of different isotopes. For ^{238}U, emissions from ^{234}Th and ^{234m}Pa are searched to quantify activity of the upper part of the chain[3] and lines from ^{214}Pb and ^{214}Bi for the sub-chain starting with ^{226}Ra up to ^{210}Pb. For ^{232}Th chain, emissions of ^{228}Ac are analyzed for the upper part and those of ^{212}Pb, ^{212}Bi and ^{208}Tl for the lower one. Concerning ^{235}U chain, only emissions from the parent isotope are taken into account; even in the cases of not detailed quantification, activities from ^{235}U are always found reasonably consistent with natural abundance.

Table 2 summarizes the measurements performed for the samples analyzed in this work, indicating material and supplier, the detector used, the size of the sample and the live time of data

[3]The low intensity of these emissions makes upper limits on activity obtained from their analysis be typically much higher than for other isotopes in the chain.

Table 2. Information on measurements performed: component and supplier, detector used, samples size (mass or number of pieces) and screening live time. The corresponding row number of table 3 where the activity values obtained for each sample are reported is also quoted.

Component, Supplier	# in table 3	Detector	Sample size	Time (d)
Cuflon, Polyflon	1	GeOroel	1876 g	24.29
Bonding film, Polyflon	2	GeAnayet	288 g	30.83
Cuflon Dice Board, Pyrecap	3	GeOroel	140 g	45.11
Kapton-Cu Dice Board, Flexiblecircuits	4	GeOroel	647 g	26.60
FFC/FCP connector, Hirose	5	Paquito	19 pc $\times$ 1.23 g/pc	6.83
P5K connector, Panasonic	6	Paquito	15 pc $\times$ 0.67 g/pc	7.58
Thermoplastic connector, Molex	7	GeLatuca	29 pc $\times$ 0.53 g/pc	17.20
Solder paste, Multicore	8	GeLatuca	457 g	44.30
Solder wire, Multicore	9	Paquito	91 g	7.74
Silver epoxy, Circuit Works	10	GeLatuca	125 g	55.11
SiPMs 1$\times$1 mm^2, SensL	11	GeAspe	102 pc $\times$ 3.4 mg/pc	41.42
SiPMs 6$\times$6 mm^2, SensL	12	GeAspe	99 pc $\times$ 96 mg/pc	59.62
NTC sensor, Murata	13	GeLatuca	1000 pc $\times$ 4.5 mg/pc	28.27
LEDs, Osram	14	GeLatuca	989 pc $\times$ 0.8 mg/pc	32.35
Plexiglas/PMMA, Evonik	15	GeLatuca	1669 g	48.87
Ta capacitor, Vishay Sprague	16	GeAnayet	277 pc $\times$ 0.64 g/pc	17.97

taking. Most of the samples were cleaned in an ultrasonic bath and with pure alcohol before starting the screening.

3. Results

#	Component	Supplier	Unit	^{238}U	^{226}Ra	^{232}Th	^{228}Th	^{235}U	^{40}K	^{60}Co	^{137}Cs
1	Cuflon	Polyflon	mBq/kg	$<$33	$<$1.3	$<$1.1	$<$1.1	$<$0.6	4.8$\pm$1.1	$<$0.3	$<$0.3
2	Bonding film	Polyflon	mBq/kg	1140$\pm$300	487$\pm$23	79.8$\pm$6.6	66.0$\pm$4.8		832 $\pm$87	$<$4.4	$<$3.8
3	Cuflon Dice Board	Pyrecap	mBq/pc	$<$ 7.6	0.28$\pm$0.08	$<$ 0.28	$<$ 0.16	$<$0.13	$<$1.2	$<$0.07	$<$ 0.06
4	Kapton-Cu Dice Board	Flexiblecircuits	mBq/pc	$<$1.3	0.031$\pm$0.004	0.027$\pm$0.008	0.042$\pm$0.004		12.1$\pm$1.2	$<$0.01	$<$0.01
5	FFC/FCP connector	Hirose	mBq/pc	$<$50	4.6$\pm$0.7	6.5$\pm$1.2	6.4$\pm$1.0	$<$0.75	3.9$\pm$1.4	$<$0.2	$<$0.5
6	P5K connector	Panasonic	mBq/pc	$<$42	6.0$\pm$0.9	9.5$\pm$1.7	9.4$\pm$1.4	$<$0.95	4.1$\pm$1.5	$<$0.2	$<$0.8
7	Thermopl. connector	Molex	mBq/pc	$<$7.3	1.77$\pm$0.08	3.01$\pm$0.19	2.82$\pm$0.15	$<$0.31	2.12$\pm$0.25	$<$0.022	0.27$\pm$0.03
8	Solder paste	Multicore	mBq/kg	$<$310	$<$2.7	$<$4.7	$<$2.5	$<$5.2	$<$13	$<$1.0	$<$1.6
9	Solder wire	Multicore	mBq/kg	$<$4900	(7.7$\pm$1.2)10^2	$<$147	$<$14		$<$257	$<$30	$<$36
10	Silver epoxy	Circuit Works	mBq/kg	$<$1.0 10^3	13.6$\pm$2.8	$<$18	$<$ 16	$<$4.5	$<$52	$<$1.9	$<$2.2
11	SiPMs 1$\times$1 mm^2	SensL	μBq/pc	$<$320	$<$2.7	$<$6.9	$<$2.0	$<$1.0	$<$16	$<$0.8	$<$2.0
12	SiPMs 6$\times$6 mm^2	SensL	μBq/pc	$<$410	$<$3.2	$<$12	$<$2.8	$<$2.5	$<$25	$<$1.2	$<$1.3
13	NTC sensor	Murata	μBq/pc	$<$96	$<$0.8	$<$0.9	$<$0.3	$<$0.3	$<$2.9	$<$0.2	$<$0.2
14	LED	Osram	μBq/pc	$<$90	1.4$\pm$0.2	3.5$\pm$0.4	3.0$\pm$0.3	$<$0.6	$<$4.0	$<$0.2	$<$0.3
15	Plexiglas/PMMA	Evonik	mBq/kg	$<$208	$<$1.3	$<$2.2	$<$1.0	$<$1.1	$<$8.1	$<$0.4	$<$0.6
16	Ta capacitor	Vishay Sprague	mBq/pc	$<$0.8	0.043$\pm$0.003	0.034$\pm$0.004	0.032$\pm$0.003	$<$ 0.010		$<$0.002	$<$0.003

Table 3: Activities measured for tracking readout components to be used in NEXT. Results reported for ^{238}U and ^{232}Th correspond to the upper part of the chains and those of ^{226}Ra and ^{228}Th give activities of the lower parts. All the activities have a global 10% uncertainty coming from the Monte Carlo estimate of the detection efficiency (see text for more details).

Table 4. Summary of activities measured for the most relevant components of the tracking readout plane and the corresponding expected background rate in the region of interest for NEXT-100 estimated by Monte Carlo simulation. As a reference, the maximum allowed activities and rate for the whole tracking plane are indicated in the first row. Last column indicates if the component has been finally accepted or not for use in NEXT-100 set-up.

Component	^{208}Tl activity	^{214}Bi activity	Background rate b (counts keV^{-1} kg^{-1} y^{-1})	Accepted
Whole plane	35 mBq	35 mBq	4×10^{-4}	
Cuflon Dice Boards	$<$0.06 mBq/pc	0.28 mBq/pc	$(1.8< b <2.1)\times10^{-4}$	No
Hirose connectors	2.3 mBq/pc	4.6 mBq/pc	4.3×10^{-3}	No
Kapton Dice Boards	0.015 mBq/pc	0.031 mBq/pc	2.8×10^{-5}	Yes
SiPMs (1×1 mm^2)	<0.03 μBq/pc	<0.09 μBq/pc	$< 0.5\times10^{-5}$	Yes
LEDs	1.1 μBq/pc	1.4 μBq/pc	0.2×10^{-5}	Yes
NTC sensors	<0.1 μBq/pc	<0.8 μBq/pc	$< 0.06\times10^{-5}$	Yes

The activity results obtained for the samples analyzed dealing with the tracking readout plane are all summarized in table 3; reported errors correspond to 1σ uncertainties including both statistical and efficiency uncertainties. The expected contribution to the background level in the region of interest of NEXT-100 from the activities of the most relevant components of the tracking plane has been evaluated by Monte Carlo simulation and is reported in table 4. In the following, each sample is described and the corresponding results discussed.

3.1 Printed Circuit Boards and cables

Printed Circuit Boards (PCBs) are commonly made of different materials and a large number of radiopurity measurements can be found in [20]. Therefore, several options have been taken into consideration for the substrate of SiPMs arrays. FR4 was disregarded because of both an unacceptable high rate of outgassing and bad radiopurity; glass fiber-reinforced materials at base plates of circuit boards are generally recognized as a source of radioactive contamination [19].

Cuflon® offers low activity levels, as shown in the measurement of samples from Crane Polyflon[4] by GERDA [28] and at [29], using both ICPMS and Ge gamma spectroscopy. As presented in [15], a measurement of Polyflon cuflon made of a 3.18-mm-thick PTFE layer sandwiched by two 35-μm-thick copper sheets was made for NEXT and results are shown in row #1 of table 3. Adhesive films to glue cuflon sheets are used to prepare multilayer PCBs; a sample of bonding films made of a polyolefin co-polymer and supplied also by Crane Polyflon were screened and results are presented in row #2 of table 3. Four cuflon DB produced by Pyrecap company using these Polyflon materials were screened. Each DB, with a surface of 79×79 mm^2 and a mass of 35 g, was made of three cuflon sheets glued with two bonding films; results are shown in row #3 of table 3, being fully consistent with the individual measurements of components. Total activity from each cuflon DB was too high for NEXT requirements, since they could produce a background

[4] http://www.polyflon.com

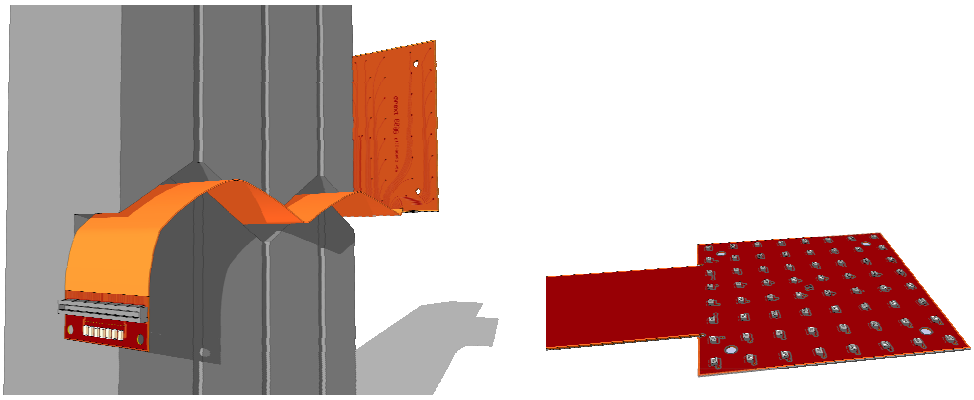

Figure 3. Left: Design of the all-in-one DB made of kapton and copper, consisting of a square part and a long, flexible tail, which allows to locate the connectors behind the inner copper shielding. Right: Detail of the square part where SiPMs and NTC sensor are fixed.

of 2.1×10^{-4} counts keV^{-1} kg^{-1} y^{-1} in the region of interest (see table 4); consequently, other option was searched for.

Components made of just kapton (like cirlex) and copper offer very good radiopurity, as shown in the measurements of kapton-copper foils in [30, 23]. Therefore, new DB produced by Flexible-circuit using only kapton, metallized copper and adhesive were analyzed. A two layer adhesiveless base substrate with polyimide coverlay on both sides, which only requires a little amount of adhesive, was chosen for the boards manufacturing. As shown in figure 3, each DB consists of a square part with 8 cm side, where SiPMs are fixed, and a long, flexible tail, which allows to locate connectors behind the inner copper shielding. The mass of each kapton DB is 16.7 g. A total of 12 units, together with residual pieces from production to increase the mass sample, were screened. Results normalized to the DB part actually exposed to the detector are presented in row #4 of table 3. Although a higher content of ^{40}K (of relevance for the study of the double beta decay mode with neutrino emission) has been observed, activities for the isotopes in the lower parts of ^{238}U and ^{232}Th chains are almost one order of magnitude lower than for cuflon DB. As shown in table 4, the quantified activity of ^{208}Tl and ^{214}Bi from DBs gives a rate of 2.8×10^{-5} counts keV^{-1} kg^{-1} y^{-1} and consequently kapton DBs have been chosen as the final option for the tracking readout substrate. The problem of ^{40}K activity has been solved in flexible flat cables made also of kapton and copper by SOMACIS[5] taking care of all the materials used; from the results of a first screening of a sample of these cables and the mass of the exposed DB, the upper limit to ^{40}K activity would be 1.4 mBq/pc. No contamination was quantified neither for isotopes in the lower parts of ^{238}U and ^{232}Th chains, which would translate to upper limits at the level of a few tenths of mBq/pc for exposed DB.

It is worth noting that the portion of cables inside the pressure vessel, transporting signals from the connectors at the end of the kapton DB towards the front-end electronics, will be made using

[5] http://www.somacis.com

the same materials that the kapton DB.

3.2 Connectors

Information on the radiopurity of different types of connectors is available at [20, 31, 32]. Different kinds of board-to-cable connectors were measured [15] and results are reported in rows #5-7 of table 3. In particular, FFC/FCP (Flexible Printed Circuit & Flexible Flat Cable) connectors supplied by Hirose[6] and similar P5K connectors from Panasonic[7] were considered, finding activities of at least a few mBq/pc for isotopes in ^{232}Th and the lower part of ^{238}U chains and for ^{40}K. Thermoplastic connectors 503066-8011 from Molex[8] were also screened, giving values slightly smaller but of the same order. Since all these connectors contain Liquid Crystal Polymer (LCP), it seems that the activity measured is related to this material. As the activity of connectors would give an unacceptable high rate in the region of interest (see table 4 for the Hirose connectors), a direct bonding of the cables to the cuflon DBs was originally foreseen; however, in the final design using the all-in-one kapton DBs, connectors are easily placed behind the inner copper shield.

3.3 Soldering materials

Different materials intended to be used to solder electronic components on boards have been analyzed [15]. A sample of lead-free SnAgCu solder paste supplied by Multicore (Ref. 698840) was screened and results are presented in row #8 of table 3. ^{108m}Ag, induced by neutron interactions and having a half-life of $T_{1/2}$ =438 y, has been identified in the paste, with an activity of (5.26$\pm$0.40) mBq/kg, while upper limits of a few mBq/kg have been set for the common radioactive isotopes; consequently, some tens of grams of the solder paste could be used without concern. Solder wire with similar composition from Multicore (Ref. 442578) was also screened (see row #9 of table 3), finding in this case a high activity of the lower part of the ^{238}U chain. An activity of ^{210}Pb of (1.2$\pm$0.4)$\times 10^3$ Bq/kg was deduced using the bremsstrahlung emission from its daughter nuclide ^{210}Bi [33].

A sample of Circuit Works Conductive Epoxy CW2400 mainly made of silver was measured. It was prepared at LSC just before screening by mixing epoxy and hardener following specifications. Results are presented in row #10 of table 3. Activity of ^{108m}Ag has been measured in this sample too at a level of (24.6$\pm$1.6) mBq/kg. Even though the use of this type of silver epoxies was finally disregarded for electronic boards, it could be used for the field cage components.

3.4 SiPMs

Although silicon is, as germanium, a very radiopure material with typical intrinsic activities of ^{238}U and ^{232}Th at the level of few μBq/kg [19], materials used in the substrate or package of the chip can be radioactive. Very low specific activities have been recently obtained by Neutron Activation Analysis for bare devices from FBK manufacturer [34]. Two samples of non-functional SiPMs from SensL[9], reported as MLP (Moulded Lead-frame Package) plastic SMT elements, were

[6] http://www.hirose.com

[7] http://www.panasonic-electric-works.com

[8] http://www.molex.com

[9] http://sensl.com

screened. One consisted of 102 units with a surface of 1×1 mm^2 each, and the other of 99 6×6 mm^2 units. Results are shown in rows #11-12 of table 3; activity has not been quantified for any isotope and upper limits have been derived. Limits per unit are very similar for both samples, but since the production process is the same and the proportion of components scales with area, results from the large 6×6 mm^2 units allow to set limits on activities per surface much more stringent. A preliminary analysis of a sample of 20 units of SiPMs of type TSV (Through Silicon Via) also from SensL, 3×3 mm^2 each and made of different materials, points to a slightly worse radiopurity; presence of ^{40}K has been quantified at a level of 1 mBq/pc. As presented in table 4, the expected background from SiPMs of type MLP is $< 0.5\times10^{-5}$ counts keV^{-1} kg^{-1} y^{-1}. Therefore, these SiPMs will be considered for NEXT.

3.5 Other components

NTC thermistors chip type from Murata Manufacturing Co. Ltd[10], to be used as temperature sensors at DB, were screened. Each unit is 1.6 mm long and 0.8 mm wide. As shown in row #13 of table 3, upper limits of a few μBq/pc have been set for the common radioisotopes.

Chip LEDs 0603 supplied by Osram[11], with blue emission at 470 nm (LBQ39E) and made with InGaN technology, were measured. Each unit has a volume of $1.6\times0.8\times0.3$ mm^3. Results are presented in row #14 of table 3; high specific activities for ^{40}K, ^{232}Th and ^{238}U chains have been quantified, despite the very small mass of the sample, which correspond to levels of a few μBq/pc. In principle, the number of LEDs to be used per DB was between one to four; but it could be reduced to only 10 units for the whole plane. Following simulations, assuming one LED and one NTC sensor per DB, the total contribution at the region of interest due to these components from the lower part of ^{238}U and ^{232}Th chains will be $< 3\times10^{-6}$ counts keV^{-1} kg^{-1} y^{-1} (see table 4).

SiPMs have high photon detection efficiency in the blue region. For this reason, they need to be coated with a wavelength shifter, to shift the UV light of the scintillation of xenon to blue, as the windows of the PMTs at the energy readout plane. TetraPhenyl Butadiene (TPB) material from Sigma Aldrich has been successfully used in NEXT prototypes and according to measurements in [32], taking into account the small quantity to be used (about 20 g for the whole tracking plane), its radiopurity is good enough. Instead of directly coating the DBs, an envisaged solution was to place quartz or PolyMethyl Methacrylate (PMMA) thin windows coated with TPB in front of DBs. A sample made of 134 PMMA sheets ($79\times79\times1.5$ mm^3 and a mass of 12.46 g each one) was screened. Material is reported as Plexiglas GS/XT from Evonik Industries AG[12]. Results are shown in row #15 of table 3, setting upper limits to the analyzed radioisotopes. Although these results are not bad, the final option is to use a quartz anode, having this material also an acceptable radiopurity [35].

In a first design of the cuflon DBs, capacitors were needed. Ceramic capacitors were disregarded for being radioactive [20]. Tantalum capacitors (Vishay Sprague 597D[13]) were screened at LSC and results are presented in row #16 of table 3; activity levels are lower than for other tantalum capacitors [20]. In addition to activities shown in table 3, the presence of ^{182}Ta (beta emitter

[10] http://www.murata.com
[11] http://www.osram.com
[12] http://www.evonik.com
[13] http://www.vishay.com

with Q=1814.3 keV and $T_{1/2} = (114.74 \pm 0.12)$ days, produced by neutron activation on ^{181}Ta) was identified. In any case, in the final design of kapton-Cu DBs no capacitor is used.

4. Conclusion

A thorough control of material radiopurity is being performed in the construction of the NEXT double beta decay experiment to be operated at LSC, mainly based on activity measurements using ultra-low background gamma-ray spectrometry with germanium detectors of the Radiopurity Service of LSC. Radiopurity information is helpful not only for the selection of radiopure enough materials, but also for the development of the detector background model in combination with Monte Carlo simulations.

The design of a radiopure tracking readout plane for the NEXT detection system, which must be in direct contact with the gas detector medium, is a challenge, since PCB materials and electronic components can typically have much higher activity levels than those tolerated in ultra-low background experiments. Selection of in-vessel components for the tracking plane has been performed in parallel to its design. SiPMs with low enough activity have been identified. Regarding the substrate for SiPMs, printed circuit boards made of kapton and copper have been chosen for their better radiopurity for ^{238}U and ^{232}Th chains in comparison with cuflon boards; even the reduction of the high content in ^{40}K measured seems possible for kapton PCBs. Since kapton is flexible, the design of all-in-one kapton boards with long flexible tails as cables has allowed in addition to place connectors, having unacceptable activities (a few mBq per piece for isotopes of the ^{238}U and ^{232}Th chains), behind the inner copper shielding. NTC thermistors acting as temperature sensors and LEDs used for calibration are also placed on the kapton boards; units fulfilling NEXT requirements have been also selected. Solder paste of acceptable radiopurity has been found and will be used to fix SiPMs, LEDs, and NTC sensors on kapton DBs.

The precise construction of NEXT-100 background model is underway [18], based on Geant4 simulation. Using the activity levels presented here, the estimated contribution of the tracking plane to the background level in the region of interest for the neutrinoless double beta decay of ^{136}Xe has been preliminarily analyzed. As it can be concluded from table 4, the upper limits or the quantified activity of ^{208}Tl and ^{214}Bi for the selected components for the tracking readout give a rate below 4×10^{-5} counts keV^{-1} kg^{-1} y^{-1}, which is only 5% of the required background level. A fruitful collaboration with SensL company has allowed to improve the sensitivity of the screening of SiPMs and then reduce considerably the upper limits derived for the activity levels and therefore its impact on the background model. The analysis of other components to be placed behind the inner copper shield or even the vessel like connectors or feedthroughs is also foreseen, although with lower priority.

Acknowledgments

We deeply acknowledge John Murphy and Carl Jackson from SensL Technologies Ltd for their efficient collaboration in the analysis of SiPMs. We very much thank also Vicenzo Mancini from SOMACIS company for the care in the development of radiopure kapton PCBs. Special thanks are due to LSC directorate and staff for their strong support for performing the measurements at

the LSC Radiopurity Service. The NEXT Collaboration acknowledges funding support from the following agencies and institutions: the European Research Council under the Advanced Grant 339787-NEXT and the T-REX Starting Grant ref. ERC-2009-StG-240054 of the IDEAS program of the 7th EU Framework Program; the Spanish Ministerio de Economía y Competitividad under grants CONSOLIDER-Ingenio 2010 CSD2008-0037 (CUP), FPA2009-13697-C04-04, and FIS2012-37947-C04; the Director, Office of Science, Office of Basic Energy Sciences of the US DoE under Contract no. DE-AC02-05CH11231; and the Portuguese FCT and FEDER through the program COMPETE, Projects PTDC/FIS/103860/2008 and PTDC/FIS/112272/2009.

References

[1] J.J. Gomez-Cadenas et al, *The search for neutrinoless double beta decay*, *Riv. Nuovo Cim.* **35** (2012) 29-98.

[2] S. R. Elliott, *Recent Progress in Double Beta Decay*, *Mod. Phys. Lett.* **A 27** (2012) 1230009.

[3] F. T. Avignone III et al., *Double Beta Decay, Majorana Neutrinos, and Neutrino Mass*, *Rev. Mod. Phys.* **80** (2008) 481.

[4] O. Cremonesi and M. Pavan, *Challenges in Double Beta Decay*, *Advances in High Energy Physics* **2014** (2014) 951432.

[5] http://www.lsc-canfranc.es

[6] J. J. Gomez Cadenas et al, *Present Status and Future Perspectives of the NEXT Experiment*, *Advances in High Energy Physics* **2014** (2014) 907067.

[7] V. Alvarez et al., *Near-Intrinsic Energy Resolution for 30 to 662 keV Gamma Rays in a High Pressure Xenon Electroluminescent TPC*, *Nucl. Instrum. Meth. A* **708** (2013) 101–114.

[8] V. Alvarez et al., *Initial results of NEXT-DEMO, a large-scale prototype of the NEXT-100 experiment*, *JINST* **8** (2013) P04002.

[9] V. Alvarez et al., *Ionization and scintillation response of high-pressure xenon gas to alpha particles*, *JINST* **8** (2013) P05025.

[10] V. Alvarez et al., *Operation and first results of the NEXT-DEMO prototype using a silicon photomultiplier tracking array*, *JINST* **8** (2013) P09011.

[11] V. Alvarez et al., *Description and commissioning of NEXT-MM prototype: first results from operation in a Xenon-Trimethylamine gas mixture*, *JINST* **9** (2014) P03010.

[12] V. Alvarez et al., *Characterization of a medium size Xe/TMA TPC instrumented with microbulk Micromegas, using low-energy γ-rays*, *JINST* **9** (2014) C04015.

[13] J.J. Gomez-Cadenas et al., *Sense and sensitivity of double beta decay experiments*, *J. Cosmol. Astropart. Phys.* **06** (2011) 007.

[14] D. Lorca et al., *Characterisation of NEXT-DEMO using xenon K_α X-rays*, *JINST* **9** (2014) P10007.

[15] V. Alvarez et al, *Radiopurity control in the NEXT-100 double beta decay experiment: procedures and initial measurements*, *JINST* **8** (2013) T01002.

[16] V. Alvarez et al, *Radiopurity control in the NEXT-100 double beta decay experiment*, *AIP Conf. Proc.* **1549** (2013) 46.

[17] T. Dafni et al, *Results of the material screening program of the NEXT experiment*, to appear in *Nucl. Phys. B (PS)*.

[18] M. Nebot-Guinot for the NEXT collaboration, *Backgrounds and sensitivity of the NEXT double beta decay experiment*, proceedings of ICHEP 2014, July 2nd to 9th, Valencia (Spain), [arxiv:1410.6699].

[19] G. Heusser, *Low-radioactivity background techniques*, *Annu. Rev. Nucl. Part. Sci.* **45** (1995) 543-590.

[20] ILIAS Database, http://radiopurity.in2p3.fr.

[21] V. Saveliev, *Silicon Photomultiplier - New Era of Photon Detection*, Advances in Optical and Photonic Devices, Ki Young Kim (Ed.) (2010).

[22] V. Alvarez et al., *Design and characterization of the SiPM tracking system of NEXT-DEMO, a demonstrator prototype of the NEXT-100 experiment*, *JINST* **8** (2013) T05002.

[23] F. Aznar et al., *Assessment of material radiopurity for Rare Event experiments using Micromegas*, *JINST* **8** (2013) C11012.

[24] Ll. A. Currie, *Limits for qualitative detection and quantitative determination. Application to radiochemistry*, *Anal. Chem.* **40** (1968) 586-377.

[25] L. Baudis et al., *Gator: a low-background counting facility at the Gran Sasso Underground Laboratory*, *JINST* **6** (2011) P08010.

[26] Ch. Hurtgen et al., *Revisiting Currie: how long can you go?*, *Appl. Rad. Isot.* **53** (2000) 45-50.

[27] S. Agostinelli et al., *GEANT4-a simulation toolkit*, *Nucl. Instrum. Meth.* **A 506** (2003) 250.

[28] D. Budjas et al., *Gamma-ray spectrometry of ultra low levels of radioactivity within the material screening program for the GERDA experiment*, *Appl. Rad. and Isot.* **67** (2009) 755.

[29] S. Nisi et al., *Comparison of inductively coupled mass spectrimetry and ultra low-level gamma-ray spectroscopy for ultra low background material selection*, *Appl. Rad. and Isot.* **67** (2009) 828.

[30] S. Cebrián et al., *Radiopurity of micromegas readout planes*, *Astropart. Phys.* **34** (2011) 354-359.

[31] C. Arpesella et al., *Measurements of extremely low radioactivity levels in BOREXINO*, *Astropart. Phys.* **18** (2002) 1-25.

[32] I. Lawson and B. Cleveland, *Low Background Counting At SNOLAB*, *AIP Conf. Proc.* **1338** (2011) 68-77.

[33] A. Nachab and Ph. Hubert, *^{210}Pb activity by detection of bremsstrahlung in ^{210}Bi beta-decay*, *Nucl. Instrum. Meth.* **B 274** (2012) 188-190.

[34] I. Ostrovskiy et al., *Characterization of Silicon Photomultipliers for nEXO*, arXiv:1502.07837 [physics.ins-det].

[35] S. Leonard et al., *Systematic study of trace radioactive impurities in candidate construction materials for EXO-200*, *Nucl. Instrum. Meth.* **A 591** (2008) 490.